Dynamic scaling of desert dunes

Sebastian Fischer
Physik Department, TU München, 85748 Garching, Germany

Michael E. Cates
SUPA, School of Physics, The University of Edinburgh, JCMB King's Buildings, Edinburgh EH9 3JZ, United Kingdom

Klaus Kroy*
Institut für Theoretische Physik, Universität Leipzig, Postfach 100920, 04009 Leipzig, Germany
and Hahn-Meitner Institut, Glienicker Straße 100, 14109 Berlin, Germany

(Received 26 November 2007; published 12 March 2008)

The shapes of shifting sand dunes of different size and under diverse environmental conditions exhibit a remarkably high degree of similarity. On this basis, a reduced shape parametrization of dunes in terms of a few characteristic parameters such as height and length is routinely applied in the geomorphological literature. In view of the *a priori* extremely high dimensionality of a freely evolving dune's state space, the justification for this common practice is, despite its alluring simplicity, all but obvious. In order to unveil the origin of the apparent reduction of complexity, we study the dynamics of (slices of) isolated dunes within the framework of the recently proposed *minimal model* of sand dune formation [K. Kroy, G. Sauermann, and H. J. Herrmann, Phys. Rev. Lett. **88**, 054301 (2002); Phys. Rev. E **66**, 031302 (2002)]. Our numerical solutions—complemented by scaling relations derived from the model equations—show that the predicted time evolution of the shape and size of dunes, in response to naturally varying conditions such as wind strength and sand supply, is subject to a similarity law, closely controlled by the instability modes of the steady-state solutions of the model equations. By this dynamical similarity, the multitude of observed shapes and time evolutions of desert dunes is traced back to a unified growth law and to the elementary scales provided by grain size and wind speed.

DOI: 10.1103/PhysRevE.77.031302 PACS number(s): 45.70.Qj

I. INTRODUCTION

Wind-blown sand creates some of the most impressive inanimate dynamic structures in nature, spanning more than four decades of length from the neat ripple patterns on beaches through dunes and draas to vast shifting dune fields swallowing roads and settlements [1,2]. On each scale, structure formation obeys similar rules [3–5], while admitting considerable shape variations [6,7]. Emerging from the subtle interplay of turbulent air flow and nonequilibrium sand transport, isolated dunes and particularly barchan dunes with their eye-catching crescent shape (see Fig. 1 for a sketch) are among the most prominent wind-shaped structures. Barchan fields form under unidirectional flow on plane bedrock, where sand supply is limited, and cover annual distances of 20–70 m while retaining an "exactitude of repetition and geometric order unknown in nature on a scale larger than that of crystalline structure" [1]. This high mobility together with the huge amount of sand that is displaced within a propagating dune makes shifting dune fields a considerable ecological and economical threat in arid regions.

Turbulent boundary layer flow over a smooth symmetric hump creates a weak symmetry breaking due to the dissipative nature of the emerging irregular flow patterns: the wind speed attains its maximum at a certain upwind distance δL from the crest, not right above it [9–11]. Since the erosive power of the wind is very sensitive to its speed, this behavior translates into deposition on the crest of a sand heap, where the wind speed is decreasing. That is, in a nutshell, the explanation why flat sand beds—much like water surfaces [12]—are unstable against the spontaneous formation of wavelike undulations if exposed to sufficiently strong winds [8,13]. (It is also what distinguishes "dunes" from "ripples," in which the dominant symmetry-breaking instability is attributed to the direct effects of bed-slope on grain transport [14].) The length δL is proportional to the dominant wavelength of the surface undulations, but essentially independent of their amplitude, so that the symmetry breaking remains present even for small amplitude perturbations [8,13].

By throttling down the sand supply to a degree where the wind flowing over a heap can no longer attain saturation with sand before reaching the crest, the deposition mechanism just outlined can be halted. Under these "unsaturated" conditions, erosion no longer switches into deposition with the decreas-

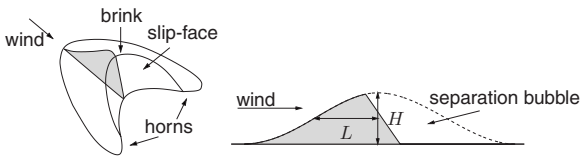

FIG. 1. Sketch of a barchan dune. Characteristic height H and length L are defined as the height and the half length at half height, respectively, of the envelope comprising the height profile and the separation bubble [8], which provides a simplistic but efficient phenomenological parametrization of the physical effects of wake zones.

*kroy@itp.uni-leipzig.de

ing wind speed at the crest. Instead, the airborne sand flux increases across the crest, which is thereby eroded. The heap shrinks and, eventually, vanishes. A wind-speed-dependent length scale ℓ_s, called the *saturation length* [15], describes the mismatch between the sand flux and the wind speed. It quantifies how far in space the actual sand flux lags behind the nominal transport capacity of the wind dictated by the local wind speed.

The so-called *minimal model* of dune formation presents both a formal and an intuitive framework that explains several important features in terms of a competition between ℓ_s and δL [8,13]. Such features include the observed systematic shape differences between dunes of different size or under different ambient conditions, the existence of a minimal dune size, and shape transitions between smooth, dome-shaped profiles and sawtooth-shaped profiles with a slip face. However, these insights are based almost entirely on *steady-state solutions* of the model equations, with periodic boundary conditions imposed to ensure exact matching of the influx and outflux of sand [8,13,16–20].

Real sand dunes, in contrast, are subject to variations of wind and other conditions, so that the influx is never exactly equal to the outflux. Here we address an intriguing and important question: *do dunes under such naturally varying conditions, which are growing or shrinking in size most of the time, still obey the similarity rules that pertain to steady states created under the artificial imposition of a constant wind speed and exact flux matching?*

Provided that the steady-state solutions were stable *attractors* of the global dynamics, this would indeed be the case: small changes in ambient conditions would cause equally small changes in dune behavior. But in fact, as we will demonstrate below, the fixed points representing these steady-state solutions are saddles and therefore unstable with respect to small perturbations in wind speed and/or influx: dunes are generically driven *away* from the steady-state solutions [8,16,17,20,21]. Despite this, we show here that the unstable solutions, which describe dunes that are either growing or shrinking, remain subject to a form of dynamical similarity. We will see that a decisive role in this is played by the *unstable manifolds* of the fixed points, which turn out to tightly constrain the dynamic evolution of both growing and shrinking dunes. The result is a rapid evolution toward a stable dune *shape*, followed by a much slower drift away from this caused by the changing *size* of the dune. By studying this effect we uncover a unified growth law for dunes of arbitrary mass under a wide range of wind and flux conditions. Crucially our approach depends only on the general form, not the details, of the minimal model equations. Strictly speaking the significance of this analysis is limited to two-dimensional dune slices $h(x,t)$, with or without slip face, along the symmetry direction of a three-dimensional dune profile. This helps to make our analysis more transparent and independent of some debatable supplementary assumptions employed in three-dimensional modeling. On the basis that three-dimensional dunes created by unidirectional wind (e.g., transverse dunes and barchans) can essentially be regarded as weakly coupled assemblies of such slices, as the lateral sand flux is typically one order of magnitude smaller than the flux along the wind direction, our results do, however, also provide important information about the full problem.

II. MINIMAL MODEL

As outlined above, the minimal model combines two major physical mechanisms into a self-contained mathematical scheme. First, the variation of the wind strength along a dune profile is expressed in terms of the shear stress (or surface friction) $\tau(x)$ exerted by the wind on the ground [9–11]. Second, the model sets up phenomenological balance equations for the hopping of grains; the impacts of airborne grains on the sand bed dislodge new grains, thereby maintaining a "granular chain reaction" known as saltation [15]. For most practical purposes these equations can be condensed into a single differential equation for the sand transport rate, or "flux," $q(x)$:

$$\ell_s \, \partial q/\partial x = q(1 - q/q_s). \tag{1}$$

This must be solved for each value of the influx q_{in}, which is the sand transport rate at the upwind boundary. The "kinetic coefficients" [8,15] ℓ_s and q_s are called the saturation length and the saturated flux, respectively. These are unique functions of the local wind strength $\tau(x)$, unless the latter falls below a threshold value τ_t such that aeolian sand transport dies out. The shape evolution follows from the solution of Eq. (1) via mass conservation: $\partial_t h = -\rho_{\mathrm{sand}}^{-1} \partial_x q$, where ρ_{sand} is the bulk sand density of the dune. Due to a strong time-scale separation, $\tau(x)$ and $q(x)$ depend only parametrically on time t via the slow evolution of the height profile $h(x,t)$.

If the coefficients ℓ_s and q_s were mere constants, Eq. (1) would reduce to the logistic equation familiar from elementary population dynamics, which is in fact a handy starting point for qualitative considerations [22]. This already captures one of the most important properties of Eq. (1), which is a "memory effect" in the sand transport: upon a sudden change of the ambient conditions (wind strength, sand supply, etc.), the actual sand transport rate $q(x)$ lags about a distance ℓ_s behind the nominal value q_s one would predict on the basis of the locally prevailing conditions alone. An intriguing implication of Eq. (1), which is solely due to these memory effects and quite insensitive to the detailed functional form of ℓ_s, is that ℓ_s sets the only characteristic length scale in the problem [8,13,23–25]. (Remember that δL is merely a fixed percentage of the overall dune length.) As a consequence, different dune profiles should almost superpose when length and height are appropriately scaled. Recent studies of steady-state solutions, obtained for fixed wind strength and periodic flux boundary conditions, have indeed supported this expectation [20]. These works show that a nontrivial, anisotropic length renormalization meshes all windward steady-state profiles onto a single master curve, in striking agreement with field observations [7,26].

III. SIZE INSTABILITY AND SHAPE ATTRACTION

The cross-sectional shape of dunes along the wind direction can therefore to an excellent approximation be parametrized by only two quantities—say, the dune's length L and

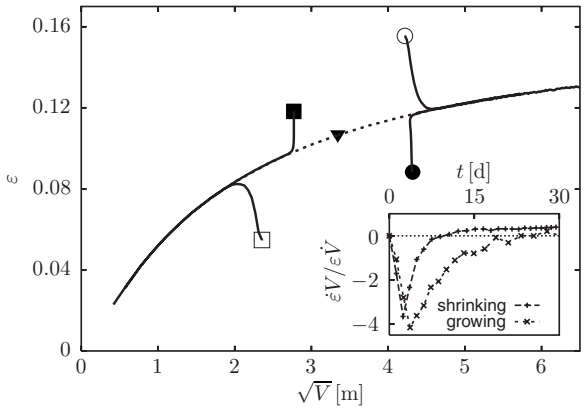

FIG. 2. "Shape attraction": stationary dome-shaped solution with its unstable manifold in the reduced V-ϵ phase space as obtained numerically from the "minimal model." Mismatched initial conditions with respect to the stationary solution (▼) under the prescribed wind and flux conditions ($\tau_0=2.2\tau_t$, $q_{in}=0.6q_{s,0}$) were created as stationary solutions corresponding to the "wrong" degree of influx saturation $q_{in}/q_{s,0}=0.4$ (○), $q_{in}/q_{s,0}=0.8$ (□) or "wrong" reference shear stress $\tau_0=1.8\tau_t$ (●), $\tau_0=2.6\tau_t$ (■), respectively. They quickly evolve (solid lines) toward the unstable manifold (dashed line). Inset: the time evolution of the ratio of the relative aspect ratio variation $\dot{\epsilon}/\epsilon$ to the relative volume variation $\dot{V}/V$ after a sudden change in ambient conditions exhibits a rapid shape adaptation followed by a slow, persisting mass evolution.

height H (see Fig. 1 for a definition) or, more pertinently, a *size parameter* $V \equiv HL$ (roughly, the dune volume per unit transverse length) and an aspect ratio or *shape parameter* $\epsilon \equiv H/L$ (roughly the average windward slope). This representation of steady-state solutions in a space of only two variables, governed in turn by only two external parameters describing ambient conditions (the overall wind strength and the influx), inspires our hypothesis that even *unsteady* solutions, which describe growing or shrinking dunes, might still be governed by a dynamical scaling law. We now elucidate the decisive role played in this by the *unstable manifolds* of the steady-state solutions, starting from an analysis of the stability properties of isolated dunes under prescribed influx. Our numerical implementation follows the procedure given in Ref. [8] where units are kept in order to get a rough sense of dimensions.

First, we note that the steady-state solutions can be represented as fixed points in our reduced phase space, which is the V-ϵ plane; see Fig. 2 (remember that in our context V denotes a volume per unit width and is hence measured in m^2). Each fixed point specifies a pair of size and shape variables V and ϵ (solid triangle in Fig. 2), describing the steady-state solution for prescribed external parameters q_{in} and τ_0. Here the overall wind speed is parametrized by τ_0, the shear stress exerted by the wind on a plane surface far from any obstacles.

Consider now a minute mismatch of ambient conditions $\{\tau_0, q_{in}\}$ to shape parameters $\{\epsilon, V\}$, achieved, say, by incrementing or decrementing the dune volume, at fixed shape, by an infinitesimal amount. As stated above, this always drives the solution away from steady-state behavior; the subsequent time evolution defines the *unstable manifold* of the fixed point. Numerically, a very small finite increment or decrement gives evolution that accurately approximates this manifold (the pair of dashed lines in Fig. 2). To further explore the reduced phase space in the vicinity of the fixed point, we also show in Fig. 2 the fate of four solutions with quite severely mismatched initial conditions. These come in two pairs, starting out as steady-state solutions corresponding to a "wrong" wind strength (solid circle and square) or "wrong" influx (open circle and square), respectively. All trajectories quickly approach the unstable manifold, which they closely follow subsequently. The inset of Fig. 2 quantifies the impression that one can discern two stages in the dynamic evolution: an initial stage dominated by the *adaptation of the shape* (quantified by ϵ) to the new ambient conditions, resulting in an evolution *toward* the unstable manifold; and a second stage dominated by the *mass change* incurred while the solution is drifting *along* the unstable manifold. Roughly speaking, one can thus identify ϵ and V with the attractive and repulsive directions of the fixed point in the reduced phase space. This explains, in hindsight, the names "size" and "shape" parameters for V and ϵ and establishes the pertinence of this parametrization. Although a precise and complete characterization would require one to address the full (infinite-dimensional) phase space of dune shapes and sizes, this low-dimensional picture qualitatively captures the numerical behavior of the minimal model in a remarkably compact and elegant way. Summarizing, although the steady-state fixed points are unstable, their unstable manifolds play, in our reduced phase space, the role of "shape attractors" for unsteady solutions describing dunes of growing or shrinking mass. In our opinion, shape attraction also underlies the (transient) convergence of numerical solutions of the minimal model with respect to the dune shape in three dimensions, where it forms the basis of the unambiguous identification of the wind- and influx-dependent minimum size of a freely evolving three-dimensional barchan dune (i.e., the smallest dune with a slip-face in its central part) [27].

To illustrate this further, a representative "phase diagram" for a given τ_0 is presented in Fig. 3. This delineates the various possible types of solution (steady-state, asymptotically shrinking and growing, dome-shaped, sawtooth-shaped) in the reduced V-ϵ phase space. Dome-shaped steady-state solutions result for small volume V and finite influx q_{in} (lower branch of the solid line) and sawtooth-shaped dunes for large V and vanishing q_{in} (upper branch of the solid line), irrespective of the initial conditions.[1] An exception occurs in the vicinity of the smallest dune with a slip-face, indicated by an open triangle, where there is hysteretic behavior: here the choice of the initial dune shape determines the type of steady-state solution obtained, even

[1]Note that the vanishing influx q_{in} in the case of a sawtooth-shaped dune is a peculiarity of the two-dimensional modeling, where all incoming sand is trapped in the slip face. In three dimensions a stationary sawtooth-shaped dune slice with nonzero influx exists due to a finite lateral sand flux which ensures that the flux balance is observed.

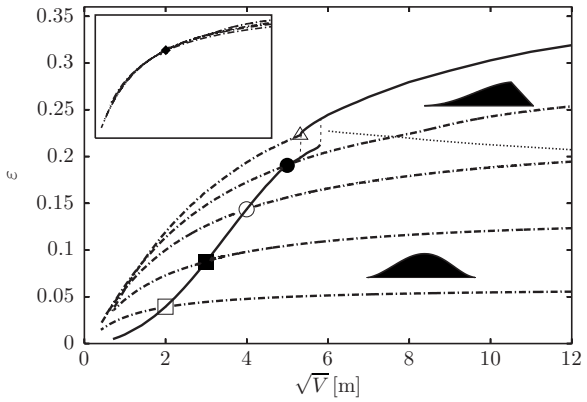

FIG. 3. Shape scaling at fixed reference shear stress $\tau_0=2.2\tau_t$. Fixed points organize the effective phase diagram in the reduced V-ϵ phase space. Fixed-point solutions are either dome shaped (lower solid line) or sawtooth shaped (upper solid line); only in the hysteretic region can both types of solutions be realized. They separate regions of growing and shrinking solutions that evolve asymptotically along the unstable manifolds (dash-dotted lines). Growing dome-shaped solutions develop a slip face upon crossing the falling dotted line. Symbols correspond to influx saturation $q_{\mathrm{in}}/q_{\mathrm{s},0}=0.86$ (□), 0.67 (■), 0.45 (○), 0.26 (●), and 0 (△). Inset: the unstable manifolds collapse onto a master curve upon rescaling as proposed in the main text.

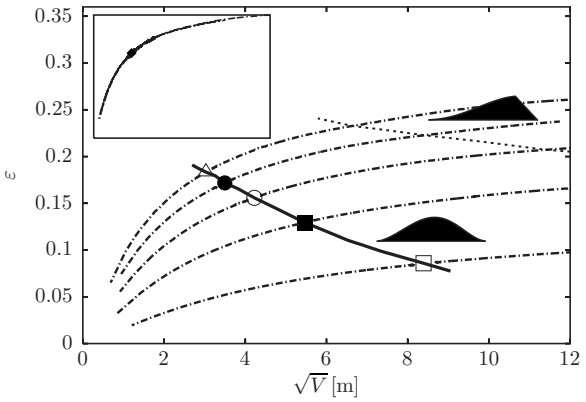

FIG. 4. Shape scaling at fixed influx saturation $q_{\mathrm{in}}/q_{\mathrm{s},0}=0.4$. Again, the fixed points organize the reduced phase space, but now all fixed-point solutions are dome shaped. They separate regions of growing and shrinking solutions that evolve asymptotically along the unstable manifolds (dash-dotted lines). Growing dome-shaped solutions develop a slip face upon crossing the falling dotted line. The symbols correspond to a reference shear stress $\tau_0=1.4\tau_t$ (□), 1.8 (■), 2.2 (○), 2.6 (●), and 3.0 (△). Inset: the unstable manifolds collapse onto a master curve upon rescaling as proposed in the main text.

under periodic flux boundary conditions. The set of all these steady-state solutions makes up a line of fixed points that divides the reduced phase space into regions of shrinking (left side) and growing (right side) dunes. Through each fixed point passes an unstable manifold (depicted for selected influx values only) which is a shape attractor for shrinking or growing dunes as they move away from the fixed point in question. Growing domelike solutions, moving rightward along such an unstable manifold, develop a slip face upon crossing the dotted line (see Ref. [21] for snapshots of the profiles). The weak slope of this line in Fig. 3 reveals a sensitive dependence of slip-face formation on the degree of influx saturation, which explains the common observation of more rounded dune shapes in regions with ample sand supply. As demonstrated in Fig. 4, an analogous picture emerges if one considers various wind speeds at fixed influx saturation $q_{\mathrm{in}}/q_{\mathrm{s},0}$.

IV. DYNAMIC SCALING

As demonstrated in the inset of Fig. 3, the unstable manifolds found for different q_{in} at the given τ_0 almost collapse onto each other on appropriate rescaling. The scaling factors here are determined empirically (viz., obtained from the fixed point solutions with the corresponding influx) and thus incorporate the full dependence of the long-time solutions on ambient conditions. However, such scaling factors can be estimated perturbatively for flat smooth profiles ($\epsilon \ll 1$), in which both the saturated flux $q_s(\tau)$ and the saturation length $\ell_s(\tau)$ are close to the reference values $q_{s,0} \equiv q_s(\tau_0)$ and $\ell_{s,0} \equiv \ell_s(\tau_0)$ obtained over a plane surface. Under these conditions, variations can be linearized in the nondimensionalized shear stress deviation τ/τ_0-1:

$$q_s/q_{s,0} \approx 1 + (\tau/\tau_0 - 1)/C(\tau_0). \tag{2}$$

Here, $C(\tau_0) \approx 1-\tau_t/\tau_0$ for not too high values of τ_0. One now considers the situation close to the windward foot of the profile, where the flux $q_s(\tau)$ must be closely matched by the influx q_{in} in order to ensure an essentially shape-invariant downwind migration. Together with the scaling $1-\tau/\tau_0 \propto \epsilon$ of the shear-stress suppression with the aspect ratio [8,13], this determines the scaling factor for the aspect ratio,

$$\epsilon \propto C(\tau_0)(1 - q_{\mathrm{in}}/q_{\mathrm{s},0}), \tag{3}$$

already anticipated in Ref. [8]. The scaling factors for height $H=\epsilon L$ and volume $V=\epsilon L^2$ follow by making use of the fact that the wind-strength dependence of the length L closely follows that of $\ell_{\mathrm{s},0}$ for flat profiles. In this vein, one also deduces the scaling of the migration speed $v \propto q_{\mathrm{s},0}/[\rho_{\mathrm{sand}} C(\tau_0)\ell_{\mathrm{s},0}]$ and the corresponding rescaling of time

$$t \propto \rho_{\mathrm{sand}} C(\tau_0)\ell_{\mathrm{s},0}^2/q_{\mathrm{s},0}. \tag{4}$$

This only depends on the wind strength and is independent of the influx, as nicely confirmed by the collapse of the numerical solutions for the time evolution of the volume of growing and shrinking profiles under various wind and sand conditions displayed in Figs. 5 and 6. Systematic deviations from scaling at large V can be attributed to shape transitions from dome-like to sawtoothlike profiles. For our two-dimensional slices, slip-face formation clearly fixes the growth rate of the profiles to $\dot{V}=q_{\mathrm{in}}/\rho_s$, as no sand can escape via the slip face. Other minor discrepancies can be traced back to additional shear-stress effects on the dune

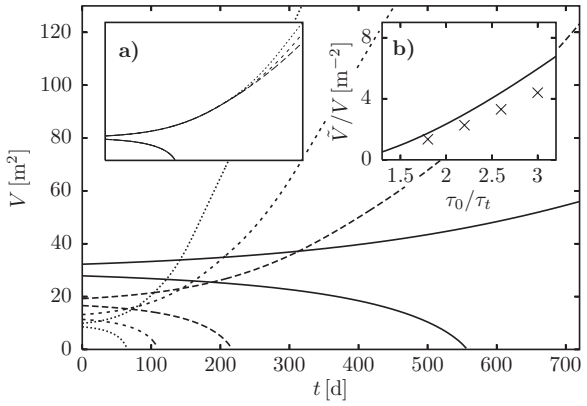

FIG. 5. Mass evolution and dynamic scaling at fixed influx saturation $q_{\mathrm{in}}/q_{\mathrm{s},0}=0.4$. Growth (shrinkage) was initiated by a slight positive (negative) volume perturbation of the stationary dome-shaped solutions obtained for various shear stresses $\tau_0/\tau_t=1.8$ (solid lines), 2.2 (long-dashed lines), 2.6 (short-dashed lines), and 3.0 (dotted lines). Inset (a): data collapse for late-time solutions achieved upon rescaling time and volume independently. Scaling is broken by shape transitions from dome-shaped to sawtooth-shaped solutions. Inset (b): the best scaling factor $\tilde{V}/V$ for V ($\times$) ($\tilde{V}$ denotes the rescaled, dimensionless volume) compared to the simple rule derived in the main text (solid line). As expected, deviations increase with increasing wind strength.

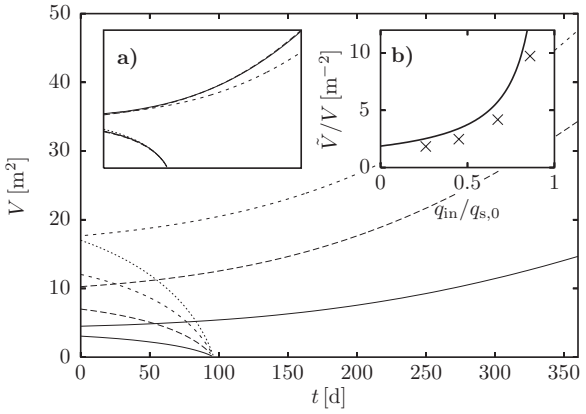

FIG. 6. Mass evolution and dynamic scaling at fixed reference shear stress $\tau_0/\tau_t=2.2$. Growth (shrinkage) was initiated by a slight positive (negative) volume perturbation of the stationary dome-shaped solutions obtained for various values of influx saturation $q_{\mathrm{in}}/q_{\mathrm{s},0}=0.86$ (solid lines), 0.67 (long-dashed lines), 0.45 (short-dashed lines), and 0.27 (dotted line). Inset (a): data collapse for late-time solutions achieved upon rescaling time and volume independently. Scaling is broken by shape transitions from dome-shaped to sawtooth-shaped solutions. Inset (b): the best scaling factor $\tilde{V}/V$ for V ($\times$) ($\tilde{V}$ denotes the rescaled, dimensionless volume) compared to the simple rule derived in the main text (solid line).

length L, not captured in $\ell_{s,0}$. In comparison to Eq. (4) the time scaling derived in Ref. [16] on purely dimensional grounds lacks the additional wind-strength-dependent factor $C(\tau_0)$ and does not capture the wind-strength dependence of our numerical data correctly.

V. CONCLUSIONS AND OUTLOOK

The above completes our prescription, based on the precepts of the minimal model of dune formation, for reducing the observed multitude of shapes and growth histories of aeolian sand dunes to a unified growth law by a dynamical rescaling transformation. Although our analysis is exclusively based on two-dimensional slices along the wind direction, we expect it to capture the qualitative behavior of propagating dunes in the field. (As mentioned at the end of the Introduction, the transverse components of the wind velocity and the sand flux that couple adjacent cross sections within a dune are typically an order of magnitude smaller than those along the wind direction.) The minimal model thus leads us to expect that the shape and dynamics of sand dunes can for many purposes be adequately represented by a simple growth curve in a dramatically reduced phase space spanned by only two state variables (size and aspect ratio). While some information and hence accuracy are necessarily lost by doing so, the ability to find a workable reduced representation of a complex system is the hallmark of successful hierarchical modeling [4].

In the case of dunes, this procedure relies on the intermediate scale invariance or homogeneity of the underlying physical mechanisms of structure formation, which in turn rests on the small grain size and the self-similarity of the turbulent wind flow. Our results justify *a posteriori* the convenient, but so far tentative characterization of desert dunes in terms of height-length relations, common in the geomorphological literature (see Ref. [23] for a recent overview), and help to unravel their sensitivity to the ambient conditions. While existing systematic investigations of the static [7,16,20] and dynamic [17,25] scaling of sand dunes support our predictions, more comprehensive measurements along these lines clearly remain highly desirable.

It would be interesting to establish to what extent the dynamical similarity rule found above might extend to the whole hierarchy [2] of self-organized structures alluded to at the start of this article and to situations, such as dunes under water or in extraterrestrial atmospheres [20,28,29], where the dominant sand transport mechanism differs from the saltation model employed in the original derivation [15] of Eq. (1), giving, e.g., potentially strongly altered functional forms for $\ell_s(\tau)$ and $q_s(\tau)$. Such expectations seem to be supported by a comparison of laboratory measurements of dunes in water with field measurements in the desert [24,25], which indicate that for submarine dunes the characteristic length scale ℓ_s in Eq. (1) is given by the grain size itself, while it is about three orders of magnitude larger for aeolian dunes because of the lower density of the driving medium. In the light of our above analysis this suggests, in particular, that there might be no direct analog of the hierarchy of aeolian ripples on aeolian dunes in subaqueous unidirectional shear flows.

Further exciting perspectives arise from the possibility to change the mass density of the grains in a controlled way [30] without invalidating the above similarity rules. This may soon permit the realization of scaled-down aeolian dunes and ripples in the laboratory, thereby removing a major obstacle for their systematic study [23,31].

ACKNOWLEDGMENTS

We would like to acknowledge discussions with B. Obermayer and M. Sperl. M.C. acknowledges the support of EPSRC Grants No. GR/S10377/01 and No. GT/T11753/01. K.K. acknowledges support by the Deutsche Forschungsgemeinschaft (DFG) through the Leipzig School of Natural Sciences: Building with Molecules and Nano-objects (BuildMoNa).

[1] R. A. Bagnold, *The Physics of Blown Sand and Desert Dunes* (Methuen, London, 1941).
[2] I. G. Wilson, Sedimentology **19**, 173 (1972).
[3] B. Hallet, Earth-Sci. Rev. **29**, 57 (1990).
[4] B. T. Werner, Science **284**, 102 (1999).
[5] H. Elbelrhiti, P. Claudin, and B. Andreotti, Nature (London) **437**, 720 (2005).
[6] R. J. Wasson and R. Hyde, Nature (London) **304**, 337 (1983).
[7] G. Sauermann, P. Rognon, A. Poliakov, and H. J. Herrmann, Geomorphology **36**, 47 (2000).
[8] K. Kroy, G. Sauermann, and H. J. Herrmann, Phys. Rev. E **66**, 031302 (2002).
[9] P. S. Jackson and J. C. R. Hunt, Q. J. R. Meteorol. Soc. **101**, 929 (1975).
[10] J. C. R. Hunt, S. Leibovich, and K. J. Richards, Q. J. R. Meteorol. Soc. **114**, 1435 (1988).
[11] W. S. Weng, J. C. R. Hunt, D. J. A. W. Carruthers, G. F. S. Wiggs, I. Livingstone, and I. Castro, Acta Mech. Suppl. **2**, 1 (1991).
[12] P. Janssen, *The Interaction of Ocean Waves and Wind* (Cambridge University Press, Cambridge, England, 2004).
[13] K. Kroy, G. Sauermann, and H. J. Herrmann, Phys. Rev. Lett. **88**, 054301 (2002).
[14] Z. Csahók, C. Misbah, F. Rioual, and A. Valance, Eur. Phys. J. E **3**, 71 (2000).
[15] G. Sauermann, K. Kroy, and H. J. Herrmann, Phys. Rev. E **64**, 031305 (2001).
[16] B. Andreotti, P. Claudin, and S. Douady, Eur. Phys. J. B **28**, 341 (2002).
[17] P. Hersen, K. H. Andersen, H. Elbelrhiti, B. Andreotti, P. Claudin, and S. Douady, Phys. Rev. E **69**, 011304 (2004).
[18] P. Hersen, Eur. Phys. J. B **37**, 507 (2004).
[19] V. Schwämmle and H. J. Herrmann, Eur. Phys. J. E **16**, 57 (2005).
[20] K. Kroy, S. Fischer, and B. Obermayer, J. Phys.: Condens. Matter **17**, S1229 (2005).
[21] S. Fischer and K. Kroy, in *Traffic and Granular Flow '05*, edited by A. Schadschneider, T. Pöschel, R. Kühne, M. Schreckenberg, and D. E. Wolf (Springer, Berlin, 2007), p. 79.
[22] R. S. Anderson, Proc.-R. Soc. Edinburgh, Sect. B: Nat. Environ. **96**, 149 (1989).
[23] B. Andreotti, P. Claudin, and S. Douady, Eur. Phys. J. B **28**, 321 (2002).
[24] P. Hersen, S. Douady, and B. Andreotti, Phys. Rev. Lett. **89**, 264301 (2002).
[25] K. Kroy and X. Guo, Phys. Rev. Lett. **93**, 039401 (2004).
[26] E. J. R. Parteli, V. Schwämmle, H. J. Herrmann, L. H. U. Monteiro, and L. P. Maia, Geomorphology **81**, 29 (2006).
[27] E. J. R. Parteli, O. Durán, and H. J. Herrmann, Phys. Rev. E **75**, 011301 (2007).
[28] E. J. R. Parteli, O. Durán, and H. J. Herrmann (unpublished).
[29] P. Claudin and B. Andreotti, Earth Planet. Sci. Lett. **252**, 30 (2006).
[30] M. Sperl and B. Behringer (private communication).
[31] O. Dauchot, F. Lechénault, C. Gasquet, and F. Daviaud, C. R. Mec. **330**, 185 (2002).